NSTU NETI

Obrabotka metallov –
Metal Working and Material Science

Journal homepage: http://journals.nstu.ru/obrabotka_metallov

Numerical and experimental investigation of heat transfer augmentation in roughened pipes

Siddhanath Nishandar [1, a], *Ashok Pise* [1, b], *Pramodkumar Bagade* [2, c, *]

[1] Department of Mechanical Engineering, Government College of Engineering, Karad, Shivaji University, Kolhapur, Maharashtra 445414, India

[2] Department of Mechanical Engineering, TSSM's Bhivarabai Sawant College of Engineering and Research (BSCOER), Narhe, Pune, Maharashtra 445414, India

[a] https://orcid.org/0000-0001-6190-3412, ✉ siddhant.nishandar04@gmail.com; [b] https://orcid.org/0009-0003-0276-8996, ✉ ashokpise@gmail.com;
[c] https://orcid.org/0000-0002-4069-1542, ✉ pramodbagade@gmail.com

ARTICLE INFO

ABSTRACT

Introduction. In many technical applications, such as thermal energy systems, chemical processing, power production, and *HVAC*, efficient heat transfer (*HT*) is essential. Research on improving *HT* performance in circular pipes is still crucial, especially when it comes to changes that cause thermal boundary layers to be disrupted and turbulence to grow. **Purpose of the work:** The purpose of this work is to thoroughly examine how convective heat transfer can be improved in circular pipes with purposefully roughened surfaces. It focuses on how surface roughness, flow pulsations, *Reynolds* number (*Re*), and heat flow rate (*Q*) affect thermal performance. **Methods of investigation.** A combination of experimental and numerical methods is employed to assess the thermo-fluid dynamics inside the pipe. Lab-scale experiments and computational fluid dynamics (*CFD*) simulations are used to investigate temperature distribution, velocity and pressure fields, turbulent kinetic energy (*TKE*), vorticity, eddy viscosity, local heat transfer coefficient (*h*), and *Nusselt* number (*Nu*). Additionally, sinusoidal pulsations are introduced at the inlet and the outlet, with regular oscillations in frequency (*f*) and amplitude (*A*), over a turbulent flow range ($6{,}753 \leq Re \leq 31{,}000$). **Results and discussion.** The results show that surface roughness enhances *HT* by significantly increasing turbulence and disrupting the thermal boundary layer. *TKE* becomes a significant factor when there is a strong correlation between higher *HT* coefficients and rising turbulence intensity. *HT* performance is further improved by introducing flow pulsations; downstream pulsation increases *Nu* by 20–22% and upstream pulsing by 16–19%. The outcomes demonstrate how effectively controlled flow pulsations and surface roughness combine to optimize heat transfer. This collaborative approach holds great potential for compact and highly efficient thermal system designs in industrial environments.

Introduction

To improve heat exchanger performance while lowering size and operating costs, several tactics have been investigated. These tactics are typically divided into two categories: passive and active. Passive methods – such as the use of finned or spirally roughened tubes – decrease the thickness of the thermal boundary layer and improve heat transfer (*HT*) by creating turbulence close to the tube wall. In recent years, these methods have drawn more attention. Active approaches, on the other hand, make use of external energy sources and include strategies like fluid pulsation, jet impingement, mechanical vibration, and the use of electrostatic fields to boost HT efficiency.

* Corresponding author
Bagade Pramodkumar M., Ph.D. (Aerospace Engineering), Professor
Department of Mechanical Engineering,
TSSM's Bhivarabai Sawant College of Engineering and Research (BSCOER),
Narhe, Pune,
445414, Maharashtra, India
Tel.: +91 9075279575, **e-mail:** pramodbagade@gmail.co

Concentrated temperature gradients can disrupt the boundary layer in both laminar and turbulent regimes, lowering thermal resistance and raising the local heat transfer coefficient, particularly in the presence of forced convection. Pulsating flow, in particular, is essential for modifying shear forces, boundary layer characteristics, and overall thermal resistance to improve HT. Consequently, there is currently significant interest in studying how pulsating flow affects convective heat transfer.

Natural pulsating flows are found in many engineering systems, including:

– eddy turbulence - chaotic disturbances inherent in turbulent flow, leading to fluctuations in velocity and pressure.

– turbomachinery - periodic variations in pressure and velocity at the compressor and turbine blades, caused by rotor rotation and flow interaction with the blades.

– transient flows - changes caused by fluctuations in the system's operational parameters.

Practical applications of pulsating flows also include:

– reciprocating internal combustion engines - intake and exhaust systems characterized by periodic flow variations due to the engine's operating cycles.

– gas turbine engines - flow oscillations caused by surge conditions.

– positive displacement pumps: the operating principle of these pumps is based on generating pulsating flow.

– human respiration - airflow that spontaneously pulsates as part of human breathing.

Although pulsating flows are sometimes perceived as undesirable disturbances, they can also enhance processes such as fuel-air mixing in combustion systems. The findings presented in the literature vary: some research indicates that heat transfer (*HT*) has improved, while others indicate that it has not improved at all or has even decreased. Important factors affecting heat transfer include surface geometry, pulsation location, *Reynolds* number (**Re**), *Prandtl* number (**Pr**), pulsation frequency (**f**), and amplitude (**A**).

Description of the problem

The heat transfer (*HT*) mechanisms in pulsating flow over roughened surfaces have not yet been fully clarified by previous studies, which are often limited to narrow parameter ranges. More research is required to determine how the placement of the pulsation source, surface roughness patterns, *Reynolds* number (**Re**), and pulsation frequency affect turbulent flow and heat transfer characteristics.

Objectives

The present study is conducted with the following objectives:

1. Investigate the effects of various factors affecting pulsating flow experimentally and numerically.
2. Establish empirical correlations based on the observed flow dynamics.
3. Analyze the effects of pulsation orientation on heat transfer.
4. Examine the differences between the performance of pulsating flow and steady-state flow.

The scope and importance of the study

Convective heat transfer is crucial for many engineering systems. Even though oscillatory flow has shown promise in enhancing heat transfer (HT), there is currently a scarcity of research on its application in thermal systems, specifically within pipe walls. Understanding the thermo-hydrodynamics of pulsating flow is crucial because higher HT leads to higher efficiency. This work fills that gap by focusing on circular pipes under sinusoidal pulsation. Future research will examine other pipe geometries and pulsation types that were not covered in this study.

Pulsating flow heat transfer (*HT*) is essential to many industrial sectors, including thermoelectric and nuclear power [5, 6], food processing [7], pharmaceuticals [8], smart buildings [9], *HVAC* [10], transportation [11], agriculture [12], petrochemicals [13], material handling [14], bulk manufacturing [15], and many more. Increased HT efficiency has led to improvements in heat exchanger design, such as the use of innovative channel forms and compact tubing. Without sacrificing functionality, these developments raise volumetric power density and use less material. *Rowin et al.* investigated *HT* prediction

on uneven surfaces [16]. *Qu et al.* [17] demonstrated that internal capillary tube roughness significantly improves startup and operational stability in micro-pulsating heat pipes (*PHPs*). Surface tension, fluid viscosity, and wall roughness all affect flow resistance, which limits stable pulse operation in fixed-diameter *PHPs* [18].

Singh et al. [19] investigated ordered roughness and pulsed flow in microchannels using 2*D* simulations. Due to enhanced vortex activity, pulsation raised the *Nusselt* number (*Nu*) by up to 32.76% regardless of roughness. They also found that the optimal pulsation frequency varies with hydraulic diameter and that rough walls result in larger pressure decreases, even with heat transfer (*HT*) improvements. *Wu* and *Cheng* [20] discovered *Nu* fluctuations in shape-variable trapezoidal silicon microchannels. In water-filled minichannels, *Lin et al.* [21] discovered that roughness heights between 18 and 96 μm improved HT. *Lu et al.* [22] confirmed that roughness raised flow resistance and *Nu* in laminar microchannel flows. *Croce et al.* [23] showed that roughness shape has a greater effect on pressure drop than *Nu*. Despite extensive research on pulsating flow dynamics, heat transfer (HT) mechanisms remain incompletely understood [24–32]. Analytical and numerical investigations in laminar flow [33–37] demonstrate localized *HT* effects, with pulsation-induced *Nu* fluctuations being dominant near the pipe entrance and decreasing downstream.

Despite extensive research on pulsating flow dynamics, the underlying heat transfer (*HT*) mechanisms remain incompletely understood [24–32]. Analytical and numerical investigations in laminar flow regimes [33–37] demonstrate localized HT effects, wherein pulsation-induced *Nu* fluctuations are most pronounced near the pipe entrance and diminish in the downstream direction.

Methodology

Fig. 1 shows the experimental setup. A copper pipe, 400 mm in length and 28 mm in diameter, serves as the test section. Flexible joints hold it in place at both ends. Four *K*-type thermocouples are embedded in axial grooves on the outer surface of the pipe and connected to a multichannel recorder via a multipoint switch to record temperature measurements. A 400 mm long nickel-chromium heater (resistivity = = 15.5 Ω/m) provides uniform heat input. Airflow is provided by a 1.5 HP centrifugal blower (800 CFM), selected for its ability to maintain turbulent flow conditions. An electrically operated solenoid valve introduces flow pulsations. Operational boundaries are influenced by static pressure, temperature rise, and *Reynolds* number (*Re*).

A flow control valve (¾" brass valve, 12V DC, 1.5 A/18 W, orifice size 25 mm, normally closed, stainless steel components), as shown in Fig. 2, is used to regulate airflow with a sub-second response time. The valve allows for adjustment of the pulsation mechanism to provide the required amplitude and frequency of pulsation.
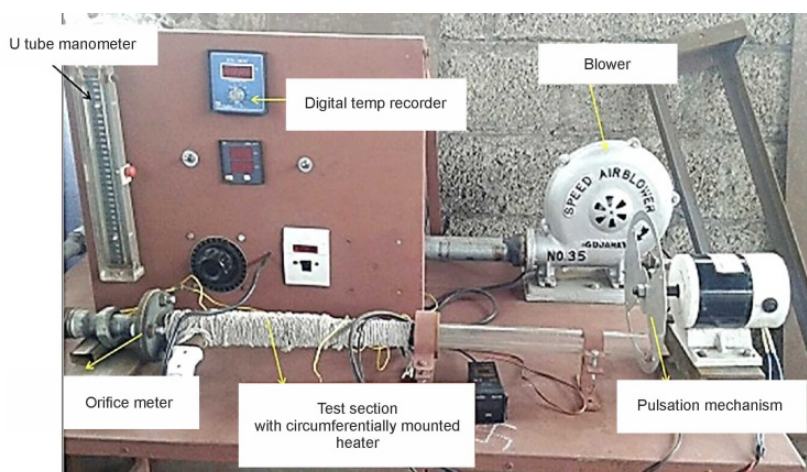

Fig. 1. Experimental set up

Fig. 2. Flow control valve

Numerical Simulation Approach

ANSYS Fluent was used for the simulations. The governing equations were the *3D Navier-Stokes* equations (Eqs. 1–6), which incorporate eddy viscosity (μ_t), strain rate (E_{ij}), and velocity components (u_i). Energy transport was governed by Eq. (7). The friction factor and theoretical *Nusselt* number (*Nu*) were determined using Eq. (8) and the *Dittus-Boelter* correlation (Eq. 9) [38–41].

$$\frac{\partial p}{\partial t} + \frac{\partial(\rho u)}{\partial x} + \frac{\partial(\rho v)}{\partial y} + \frac{\partial(\rho w)}{\partial z} = 0 \tag{1}$$

$$u\frac{\partial u}{\partial x} + v\frac{\partial u}{\partial y} + w\frac{\partial u}{\partial z} = -\frac{1}{\rho}\frac{\partial p}{\partial x} + \mu\left(\frac{\partial^2 u}{\partial x^2} + \frac{\partial^2 u}{\partial y^2} + \frac{\partial^2 u}{\partial z^2}\right) \tag{2}$$

$$u\frac{\partial v}{\partial x} + v\frac{\partial v}{\partial y} + w\frac{\partial v}{\partial z} = -\frac{1}{\rho}\frac{\partial p}{\partial y} + \mu\left(\frac{\partial^2 v}{\partial x^2} + \frac{\partial^2 v}{\partial y^2} + \frac{\partial^2 v}{\partial z^2}\right) \tag{3}$$

$$u\frac{\partial w}{\partial x} + v\frac{\partial w}{\partial y} + w\frac{\partial w}{\partial z} = -\frac{1}{\rho}\frac{\partial p}{\partial z} + \mu\left(\frac{\partial^2 w}{\partial x^2} + \frac{\partial^2 w}{\partial y^2} + \frac{\partial^2 w}{\partial z^2}\right) \tag{4}$$

$$\frac{\partial p(\rho k)}{\partial t} + \frac{\partial(\rho k u_i)}{\partial x_i} = \frac{\partial}{\partial x_j}\left[\frac{\mu_t}{\sigma_k}\frac{\partial k}{\partial x_j}\right] + 2\mu_t E_{ij} E_{ij} - \rho\varepsilon \tag{5}$$

$$\frac{\partial p(\rho k\varepsilon)}{\partial t} + \frac{\partial(\rho\varepsilon u_i)}{\partial x_i} = \frac{\partial}{\partial x_j}\left[\frac{\mu_t}{\sigma_s}\frac{\partial\varepsilon}{\partial x_j}\right] + C_{1s}\frac{\varepsilon}{k}2\mu_t E_{ij} E_{ij} - C_{2s}\rho\frac{\varepsilon^2}{k} \tag{6}$$

$$\frac{\partial}{\partial x}\left(k\frac{\partial T}{\partial x}\right) + \frac{\partial}{\partial y}\left(k\frac{\partial T}{\partial y}\right) + \frac{\partial}{\partial z}\left(k\frac{\partial T}{\partial z}\right) + q_v = \rho C_p\frac{\partial T}{\partial t} \tag{7}$$

$$f = \frac{\Delta P}{\dfrac{(L/D)\rho V^2}{2}}; \qquad V = \frac{\dot{m}}{\rho\pi D^2/4} \tag{8}$$

$$Nu = 0.023 Re^{0.8} Pr^{0.4} \tag{9}$$

Mesh Generation

Mesh quality significantly impacts accuracy. A near-orthogonal grid with $y^+ = 0.5$ (spacing $y = 1.3628\times10^{-5}$) ensures accurate wall resolution [42]. The structured mesh consisted of 1,283,136 nodes. Fig. 3 shows a cross-sectional view of the mesh. Velocity inlet conditions included a constant uniform profile for validation and a sinusoidal pulsing profile for dynamic cases, as defined by $V = U_0[1 + A\sin(2\pi f t)]$, where *A* denotes amplitude, *f* frequency, *t* time, and U_0 mean velocity. A heat flux was applied at the wall, and a pressure outlet condition was established at the pipe exit.

Fig. 3. Meshing at the cross section

Boundary Conditions

The following boundary conditions were applied:

1. A pulsating velocity profile was imposed at the inlet using a user-defined function for sinusoidal velocity input.
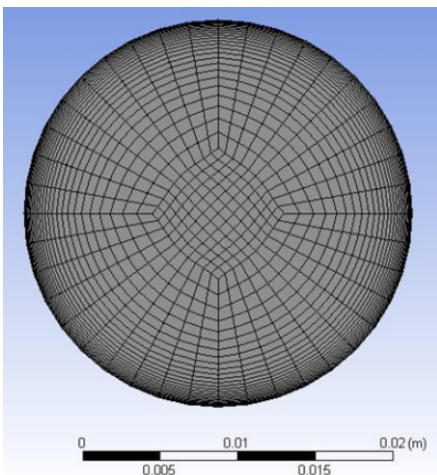
2. A constant heat flux boundary condition was applied to the pipe wall.

3. A pressure outlet boundary condition was applied at the pipe exit.

The **k-ε** turbulence model was used to resolve turbulence effects.

Validation

The present study was validated against the results of *Elshafie et al.* [43], who investigated pulsating turbulent flow (10,000 ≤ **Re** ≤ 40,000; 6.6–68 Hz) in heated pipes. Numerical accuracy was confirmed by Fig. 4, which demonstrates excellent agreement in the average *Nusselt* number (**Nu**) between the present simulations and those of *Elshafie et al.*

Fig. 5 depicts the transient variations in the surface heat transfer coefficient (**h**). The fluctuations stabilize after **t** = 2.5 s; therefore, **t** = 6 s was deemed sufficient for steady-state calculations. In all cases, **h** increases with **Re**.
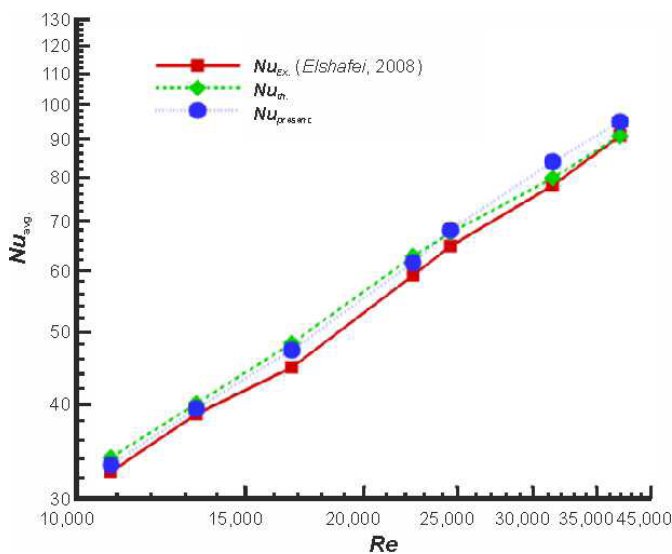

Fig. 4. Comparison of the average *Nusselt* number with the theoretical and experimental results of *Elshafie* [43]
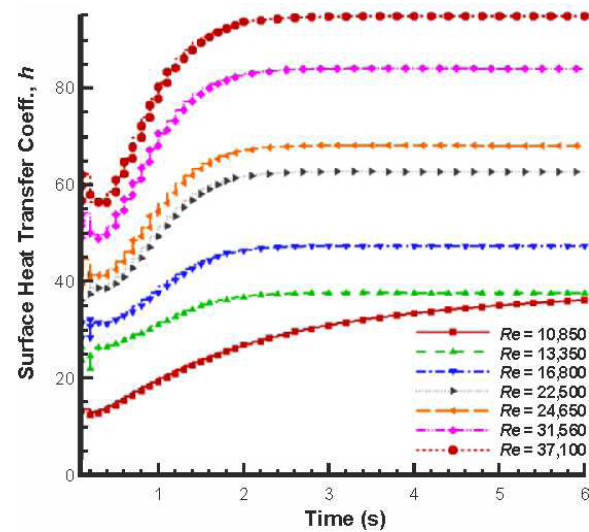
Fig. 5. Surface *HT* coefficient (**h**) obtained for different **Re**

Effects of Surface Roughness

Surface roughness enhances heat transfer (*HT*) by disrupting the thermal boundary layer [44], although it also increases pressure drop [45, 46]. Due to the complexity of the phenomena, extensive experimental research is required [47]. *MacDonald et al.* [48] demonstrated the impact of roughness on drag using direct numerical simulation (*DNS*) across sinusoidal surfaces ($k^+ = 10$, $\lambda = 0.05$–0.54). *Meyer et al.* [49] reported that roughness increases *HT* in laminar flow but has a negligible influence in turbulent regimes. *Abdelfattah et al.* [56] investigated 48-element impinging jets with hemispherical, droplet, and cylindrical roughness elements; cylinders enhanced *HT*, while droplets reduced drag.

Wall roughness affects momentum and energy transport [57]. Investigations of roughened pipes indicate that the log-law behavior is altered by a roughness function f_r, based on the roughness height **Ks+**. Equation (10) is used to account for roughness in the velocity profile, where **k** = 0.4187 (*von Karman* constant). *ANSYS Fluent* classifies hydrodynamically smooth, transitional, and completely rough regimes based on the *Cebeci-Bradshaw* method, using **ΔB** and **Ks+**.

$$\frac{u_p u^*}{\tau_w / \rho} = \frac{1}{k} \ln\left(E \frac{\rho u^* y_p}{\mu} \right) - \Delta B \tag{10}$$

Results and Discussion

Elshafie et al. [43] experimentally studied pulsating turbulent airflow in a heated pipe under constant heat flux, a configuration relevant to modern industrial heat transfer applications. They examined pulsation frequencies ranging from 6.6 to 68 Hz and *Reynolds* numbers (**Re**) from 10,000 to 40,000. Their findings demonstrated that the *Nusselt* number (**Nu**) was significantly influenced by both Re and frequency (**f**), particularly in the entrance region, where changes were more pronounced than in the fully developed zone. The downstream position of the oscillator near the pipe exit affected the distribution of local heat transfer (*HT*).

In this study, analogous investigations were conducted for **Re** = 13,350 to 37,100. Centerline velocity and total pressure increased with increasing **Re**, while the wall surface temperature decreased. These results are summarized in Table 1, which demonstrates that turbulent kinetic energy (*TKE*) and vorticity consistently increase with **Re**. Fig. 6 shows velocity profiles for **Re** = 37,100 under upstream pulsation, downstream pulsation, and no pulsation ($A = 0.2, f = 6.7$). The pulsing cases exhibit only slight variations in vorticity and lower velocities compared to the baseline (no pulsation) case. These patterns indicate that while pressure, velocity, *TKE*, and ω increase with increasing **Re**, surface temperature decreases. Consequently, **h** and **Nu** increase with **Re**, supporting the validity of the numerical method and exhibiting good agreement with theoretical and experimental findings from *Elshafie et al.* [43].

Table 1

Flow properties for various *Re* values

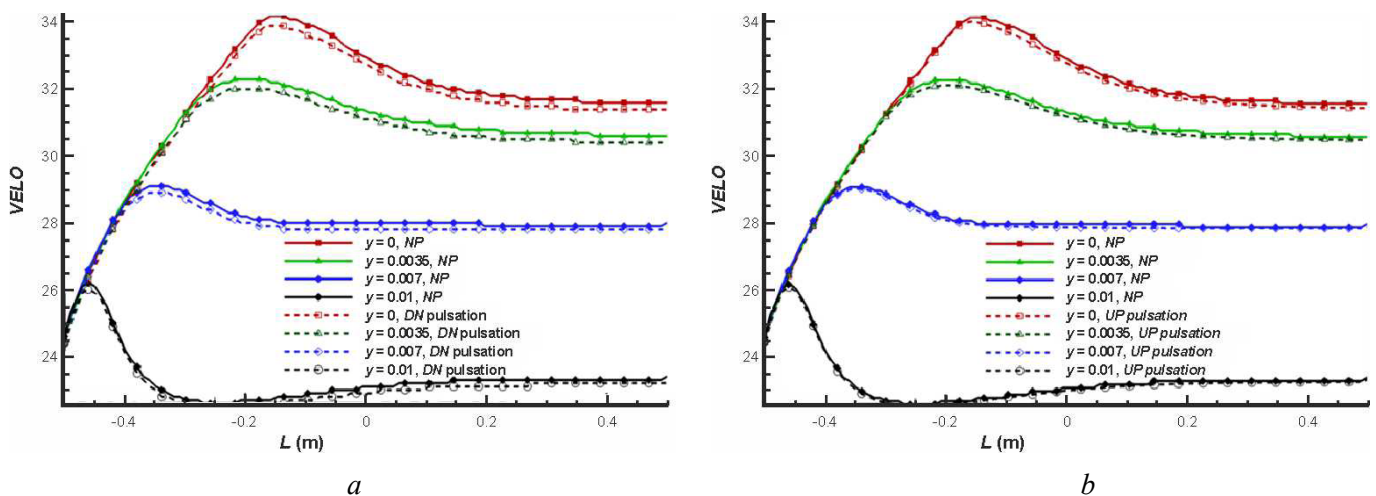| *Re*	V_{mean} (m/s)	V_{max} (m/s)	T_{max} (K)	Press. (Pa)	*TKE*	ω (s^{-1})
10,850	7.1313	10.3	329	115	1.15	1.000
13,350	8.7745	12.5	325	160	1.6	1.250
16,800	11.0420	15.6	322	255	2.7	1.600
22,500	14.7885	20.8	320	465	5	2.100
24,650	16.2016	22.6	318	552	6	2.300
31,560	20.7433	28.8	316	925	10	2.800
37,100	24.3846	33	314.2	1.300	15	3.200

a

b

Fig. 6. Comparison of velocity (**V**) profiles along the pipe length for **Re** = 37,100, under steady-state (without pulsations) and pulsating flow conditions ($A = 0.2, f = 6.7$):

a – DN pulsation = downstream pulsation; *b* – UP pulsation = upstream pulsation

Effect of location of pulsation

This section reports the effects of pulsation location. Two cases were considered:
– pulsation located downstream of the flow.
– pulsation located upstream of the flow.

Pulsation located at the downstream of the flow

Fig. 7 illustrates the increase in the mean heat transfer (*HT*) coefficient with increasing **Re** and heat input (**Q**). The enhancement ranges from 20% to 27% at ***f*** = 3.33 Hz and **Q** = 100 W, and from 30% to 36% at ***f*** = 1 Hz. Tables 2 and 3 present values of h and **Nu** for various **Re** and **Q** without pulsation. As **Re** and **Q** increase, **Nu** increases steadily, indicating improved *HT* performance.

Fig. 7. Heat transfer as a function of **Re** at varying heat input, with pulsation frequencies of ***f*** = 1 Hz and ***f*** = 3.33 Hz at downstream pulsation
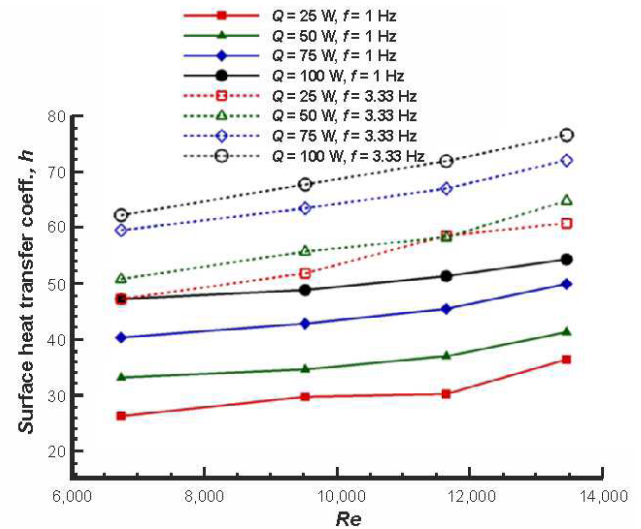
Table 2

Surface HT coefficient (*h*) at different *Re* and heat input without pulsation

Experimental heat transfer coefficient, *h*				
Re	*Q* = 25 W	*Q* = 50 W	*Q* = 75 W	*Q* = 100 W
6,753	22.1	33.04	40.25	47.13
9,504	27.92	34.48	42.77	48.74
11,618	32.11	36.88	45.4	51.26
13,414	35.53	41.19	49.89	54.29

Table 3

Variations in *Nu* with *Re* at different heat input without any pulsation

Nusselt number, *Nu*				
Re	*Q* = 25 W	*Q* = 50 W	*Q* = 75 W	*Q* = 100 W
6,753	23.43	31	37	44
9,504	29.59	32	40	45
11,618	34.04	34	42	48
13,414	37.66	38	46	50

Nu demonstrably improves with increasing heat input. The findings indicate that as *Re* and heat input increase, the mean heat transfer coefficient (h_{mean}) also increases. At f = 1 Hz, a 17–23% increase in the heat transfer (*HT*) coefficient is observed at *Q* = 100 W.

Pulsation located at the upstream of the flow

Similarly, upstream pulsation enhances heat transfer (*HT*) as *Re* and *Q* increase. At *Q* = 100 W and f = 1 Hz, the *HT* enhancement ranges from 22% to 26%, while at f = 3.33 Hz, it ranges from 29% to 33%. The generally higher *Nu* values observed under downstream pulsation, as shown in Tables 4 and 5, suggest its superior *HT* effect.

Table 4

Nu at different heat inputs with pulsation frequency, f = 1Hz and 3.33Hz when pulsating mechanism is mounted downstream

Reynolds number	Nusselt number, Nu							
	f = 1.0 Hz				*f = 3.33 Hz*			
Re	25 W	50 W	75 W	100 W	25 W	50 W	75 W	100 W
6,753	31	34	40	46	44	47	55	58
9,504	33	35	43	49	48	52	62	67
11,618	36	38	47	51	54	54	62	67
13,414	42	45	51	55	56	60	67	71

Table 5

HT Coefficient vs. Reynolds Number at Various Heat Inputs for Pulsation Frequencies f=1Hz and 3.33 Hz when pulsating mechanism is mounted upstream

Reynolds number	Nusselt number, Nu							
	f = 1.0 Hz				*f = 1.0 Hz*			
Re	25 W	50 W	75 W	100 W	25 W	50 W	75 W	100 W
6,753	26	32	38	44	37	42	48	54
9,504	29	34	40	47	41	43	53	56
11,618	29	35	43	49	44	48	56	60
13,414	34	39	48	52	52	53	61	63

Effects of pulsation frequency

Table 6 shows that increasing the pulsation frequency (*f*) from 1 Hz to 3.33 Hz significantly increases the experimental heat transfer coefficient ($h_{expt.}$) and the experimental Nusselt number ($Nu_{expt.}$). For instance, at *Re* = 6753 during downstream pulsation, $h_{expt.}$ rises from 32.91 to 47.15, and $Nu_{expt.}$ rises from 30.96 to 44.36. Similarly, at *Re* = 13,414 and f = 3.33 Hz, $h_{expt.}$ and $Nu_{expt.}$ reach 60.75 and 57.15, respectively.

Figs. 8, *a–d* illustrate the relationship between the *Reynolds* number (*Re*), heat input (*Q* = 25 W and 100 W), pulsation frequency (1 Hz, 3.33 Hz), pulsation location (upstream, downstream), the surface heat transfer coefficient (*h*), and the *Nusselt* number (*Nu*). Higher *Re* improves heat transfer at both heat inputs. In all cases, the 3.33 Hz pulsation produces the highest *h* and *Nu* values, particularly with downstream pulsation. Downstream pulsation consistently outperforms upstream pulsation. Both frequency and *Re* enhance thermal performance, with more pronounced effects at higher heat inputs (100 W). These trends indicate that pulsation settings are crucial for optimizing heat transfer.

Table 6

Experimental HT Coefficient and *Nu* for Different *Re*s and Frequencies
for *Q* = 25 *W*. *DS*= downstream; *US*=upstream

Reynolds number	$h_{expt.}$				$Nu_{expt.}$			
	f = 1.0 Hz		f = 3.33 Hz		f = 1.0 Hz		f = 3.33 Hz	
Re	DS	US	DS	US	DS	US	DS	US
6753	32.91	28.21	47.15	39.99	30.96	26.54	44.36	37.62
9504	35.9	30.97	51.79	43.88	33.77	29.13	48.72	41.28
11618	38.53	31.59	58.5	47.15	36.25	29.72	55.03	44.36
13414	45.13	36.31	60.75	56.41	42.46	34.16	57.15	53.07

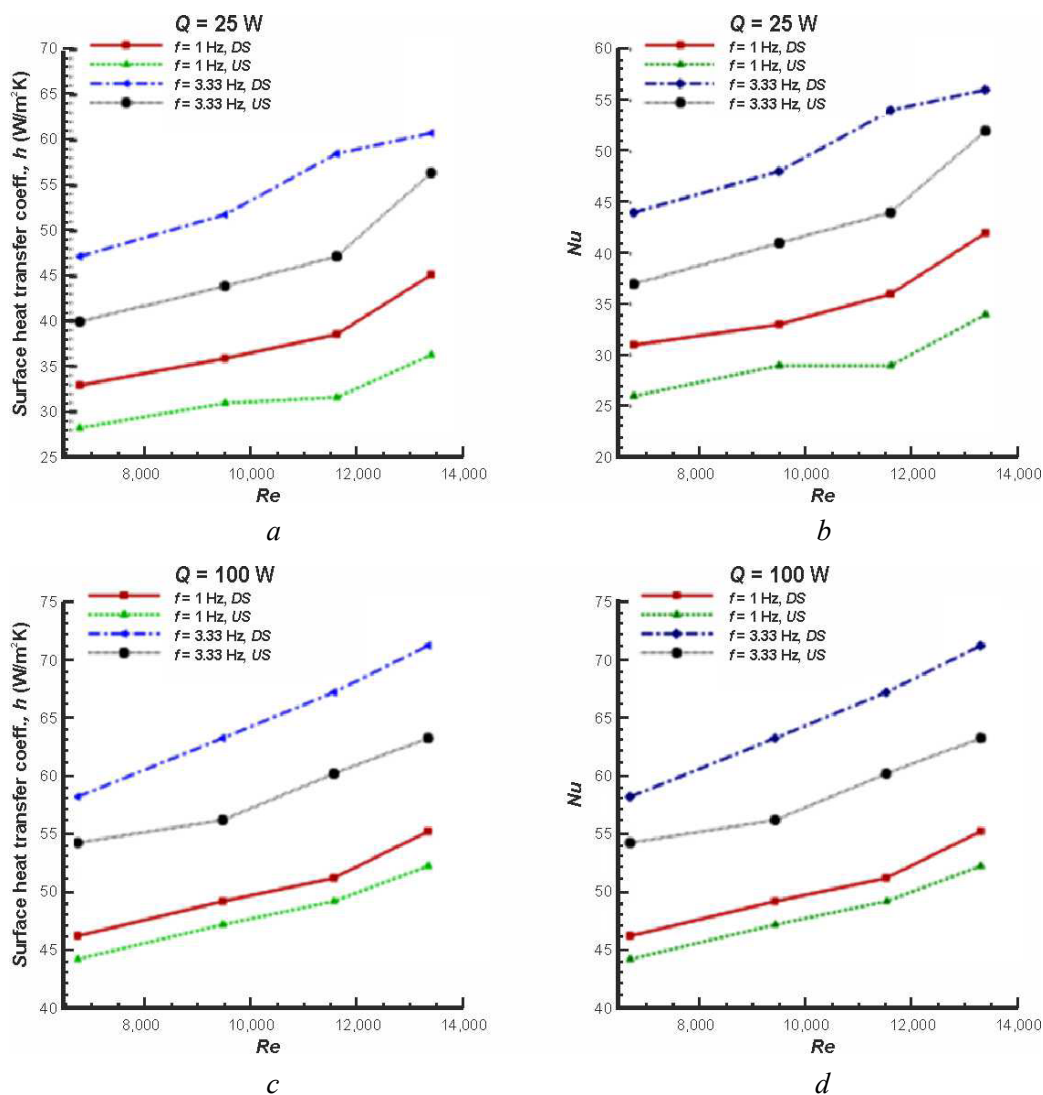*Fig. 8.* Changes in *Nu* and *h* values as a function of *Re* for various pulsation
frequencies at heat inputs of *Q* = 25 W and *Q* = 100 W

Numerical Results

Although the heat transfer (*HT*) coefficients and *Nusselt* number (*Nu*) values are derived from experiments, simulations provide a better understanding of the influencing flow mechanics. Fig. 9 displays vorticity contours under upstream pulsation for *Re* = 6753, *Q* = 954 W/m², *A* = 0.1, and *f* = 1 Hz. Shear-

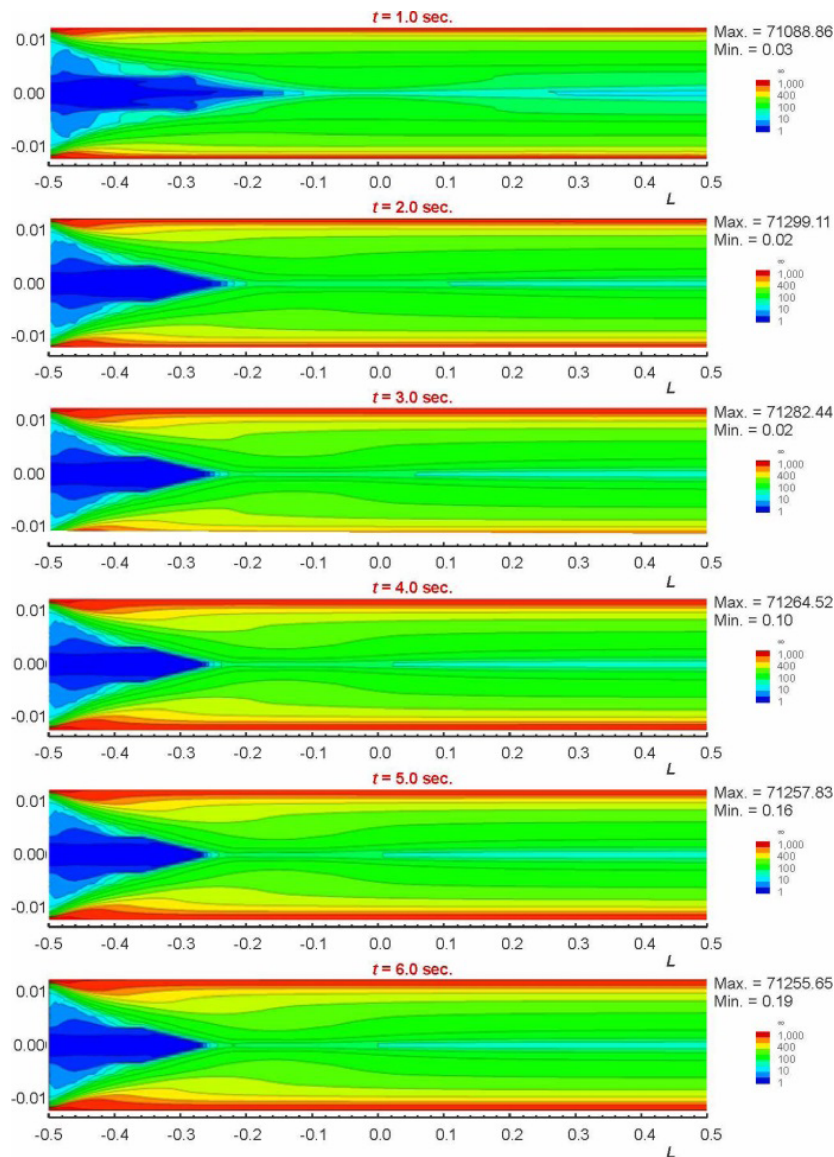*Fig. 9.* Velocity contour plots for **Re** = 6,753, heat input **Q** = 954 W/m², pulsation amplitude **A** = 0.1, pulsation frequency **f** = 1 Hz at downstream pulsation

induced turbulence is evidenced by vorticity peaks near the walls. Flow disturbances are evident near the core, and their impact diminishes beyond **L** = −0.25 m.

Fig. 10 compares the velocity contours under upstream and downstream pulsation. In the upstream case, a longer high-velocity region extends toward the pipe exit, indicating a more widespread pressure drop and increased turbulence. Conversely, downstream pulsation localizes the high-velocity region, which may lead to concentrated pressure zones and non-uniform *HT*.

Fig. 11 displays the pressure contours at **t** = 6 s. The peak pressure is higher downstream (63.21) compared to upstream due to the downstream pulsation, suggesting localized acceleration effects. Fig. 12 displays the turbulent kinetic energy (*TKE*) contours for upstream pulsation from **t** = 1 s to 6 s. *TKE* increases from 0.55 to 0.92 over time, indicating growing turbulence that enhances *HT*. The persistent and significant symmetry of the distribution promotes uniform *HT*.

Although turbulent kinetic energy (*TKE*) development initiates and concentrates more rapidly near the boundaries, *TKE* increases overall, which aligns with the observed higher local heat transfer (*HT*). The symmetry and rapid increase in turbulence observed with downstream pulsation confirm its effectiveness in enhancing convective *HT*.
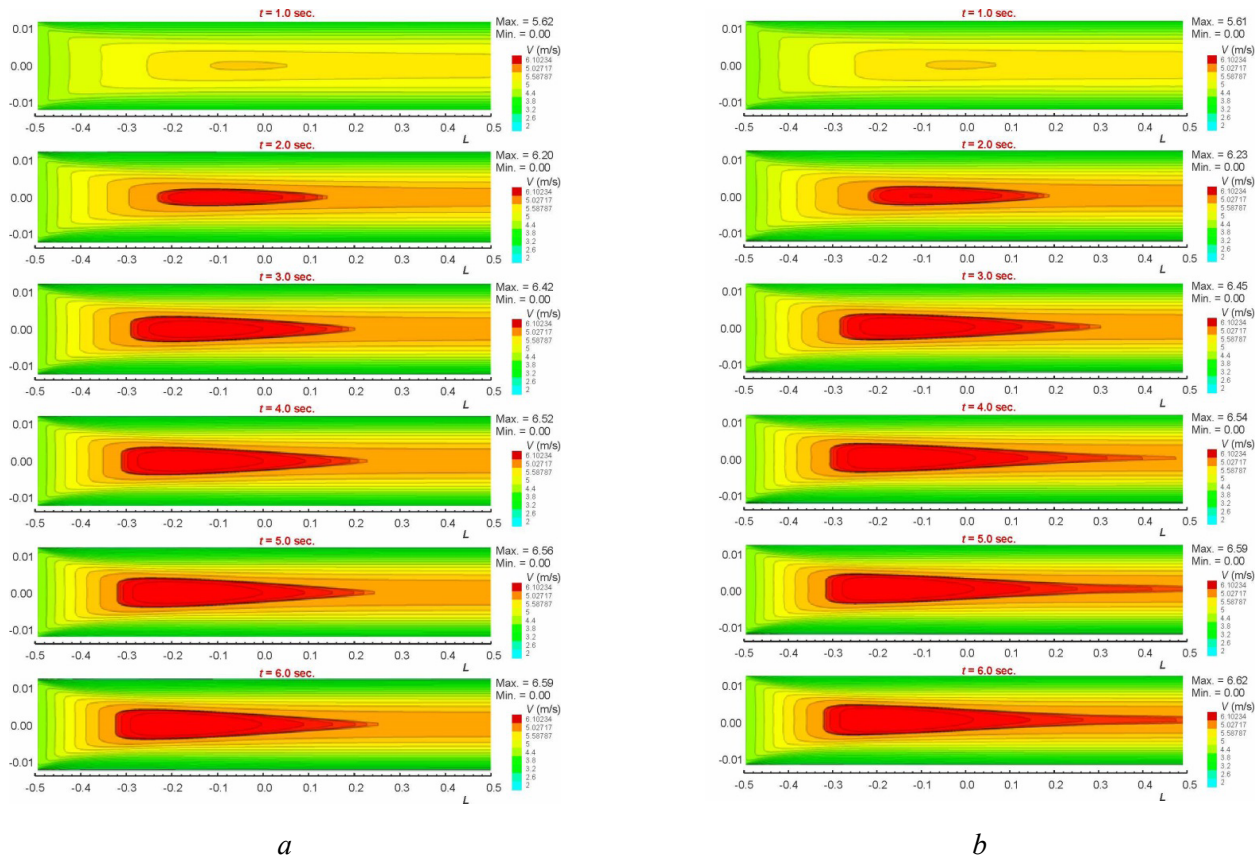
a   *b*

Fig. 10. Comparison of velocity contours for $\boldsymbol{Re}$ = 6,753, heat input $\boldsymbol{Q}$ = 954 W/m², pulsation amplitude $\boldsymbol{A}$ = 0.1, pulsation frequency $\boldsymbol{f}$ = 1 Hz at downstream pulsation (left) and upstream pulsation (right)

a   *b*
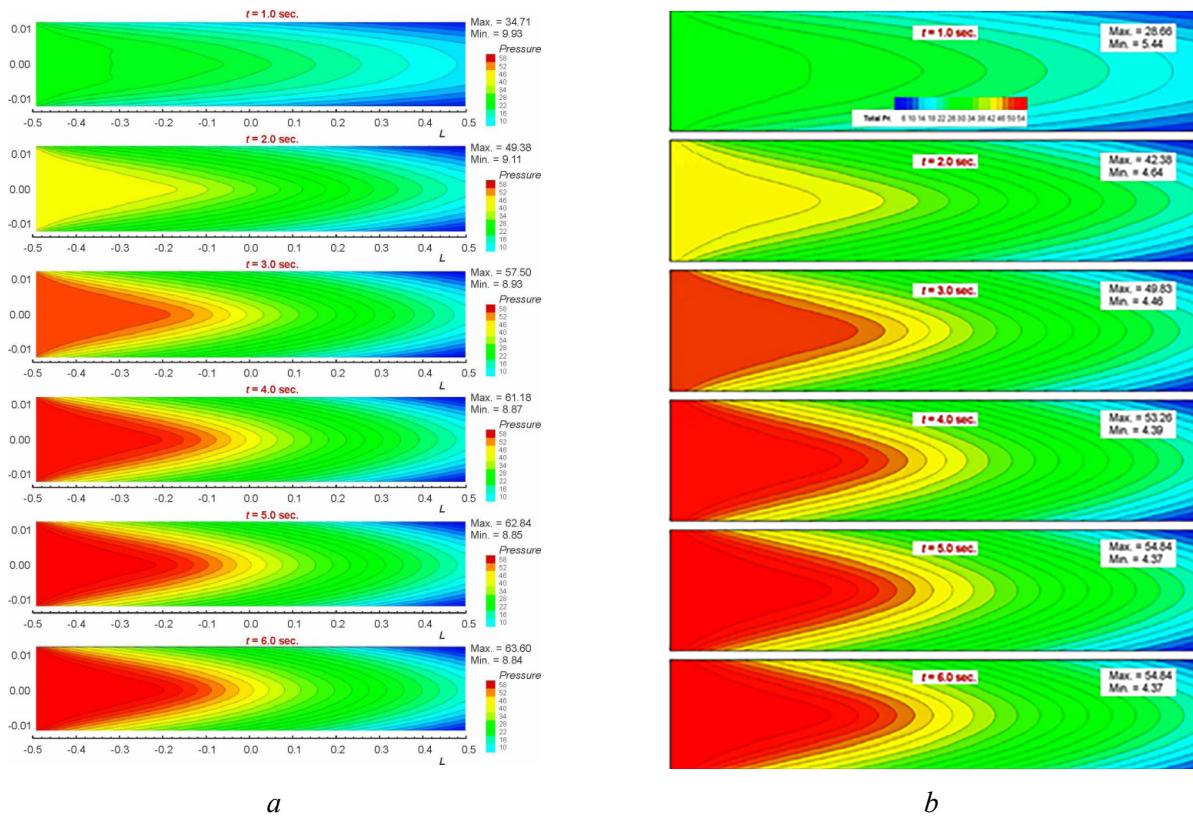
Fig. 11. Pressure contour plots in mid $\boldsymbol{y}$-plane for $\boldsymbol{Re}$ = 6,753, heat input $\boldsymbol{Q}$ = 954 W/m², pulsation amplitude $\boldsymbol{A}$ = 0.1, pulsation frequency $\boldsymbol{f}$ = 1 Hz at downstream pulsation (left) and upstream pulsation (right)
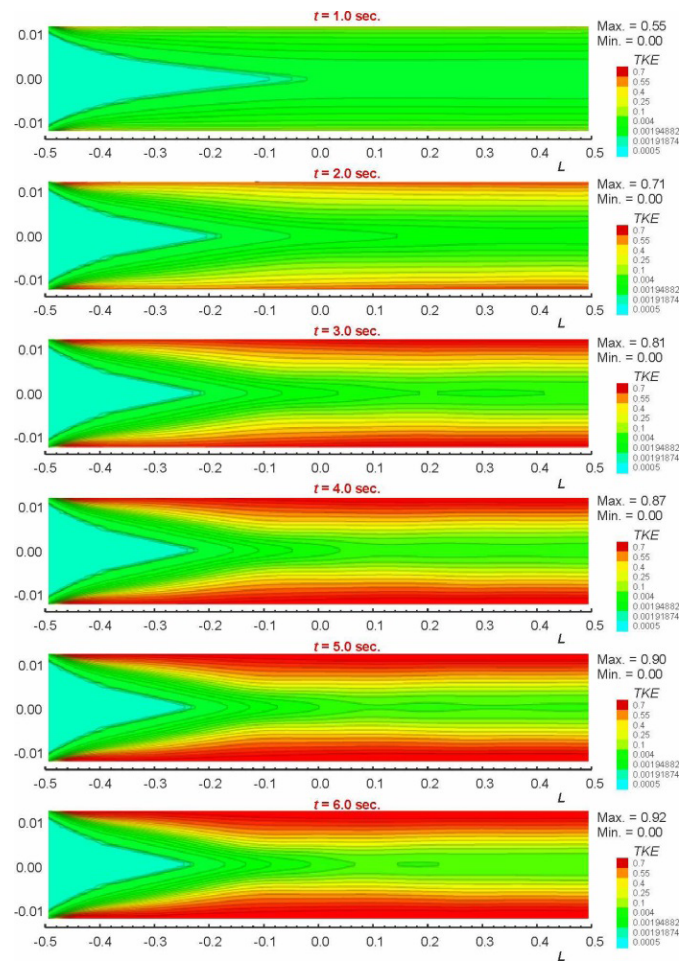
Fig. 12. Turbulent kinetic energy (*TKE*) contour
plots in the mid *y*-plane for ***Re*** = 6,753, heat input
Q = 954 W/m², pulsation amplitude ***A*** = 0.1, pulsation
frequency ***f*** = 1 Hz at upstream pulsation

These results demonstrate that pulsation, particularly when applied downstream, significantly enhances HT through increased turbulence, vorticity, and velocity variations. The primary mechanisms contributing to improved heat transport in pulsating flows are enhanced eddy formation and the generation of shear layers.

Conclusion

The enhancement of heat transfer (*HT*) in a circular pipe with surface roughness under turbulent flow conditions was investigated using a combined experimental and computational approach. The study focused on the effects of surface roughness, pulsation frequency (***f***), *Reynolds* number (***Re***), heat input (***Q***), and amplitude (***A***) on *HT* characteristics. Key parameters evaluated included velocity, pressure, and temperature distributions, turbulent kinetic energy (*TKE*), vorticity, eddy viscosity, the surface *HT* coefficient (***h***), and the *Nusselt* number (***Nu***). The following key conclusions can be drawn from the results:

1. TKE as a driver of HT enhancement:

a) *TKE* is critical for the production and sustenance of turbulence, which dominates the pulsating heat transfer mechanism.

b) Increased *TKE* strengthens fluid-wall interactions, enhancing convective *HT*, particularly with downstream pulsation as observed in this study.

c) These results align with those of previous studies [2, 3, 4], even those that did not consider roughness effects [60].

2. Impact of pulsating flow:

a) Pulsation, whether applied upstream or downstream, significantly affects turbulence parameters, with the downstream configuration exhibiting a more pronounced effect.

b) For $6753 \leq Re \leq 31000$, downstream pulsation enhanced *HT* by 20%–22%, while upstream pulsation improved *HT* by 16%–19%.

c) Pulse intensity, governed by *f* and *A*, influences the extent of turbulence penetration. No single *f* and *A* combination consistently optimizes *HT* enhancement. Future work will focus on optimization studies to determine optimal parameter combinations.

3. Future directions:

a) Future studies should investigate other fluids with varying viscosities and *Prandtl* numbers, such as water and oil.

b) Analyses should be extended to non-circular pipe geometries, such as finned or rectangular channels.

c) *HT* for non-*Newtonian* fluids under pulsating flow should be analyzed for applications in the food and pharmaceutical industries.

d) Future work should combine advanced *CFD* with experimental validation to achieve reliable predictive modeling and optimization.

In conclusion, this study demonstrates that the synergistic combination of surface roughness and pulsating flow effectively enhances *HT* performance, providing a promising approach for improving industrial heat exchanger applications.

References

1. Ye Q., Zhang Y., Wei J. A comprehensive review of pulsating flow on heat transfer enhancement. *Applied Thermal Engineering*, 2021, vol. 196, p. 117275. DOI: 10.1016/j.applthermaleng.2021.117275.

2. Yang B., Gao T., Gong J., Li J. Numerical investigation on flow and heat transfer of pulsating flow in various ribbed channels. *Applied Thermal Engineering*, 2018, vol. 145, pp. 576–589. DOI: 10.1016/j.applthermaleng.2018.09.041.

3. Duan D., Cheng Y., Ge M., Bi W., Ge P., Yang X. Experimental and numerical study on heat transfer enhancement by flow-induced vibration in pulsating flow. *Applied Thermal Engineering*, 2022, vol. 207, p. 118171. DOI: 10.1016/j.applthermaleng.2022.118171.

4. Shang F., Fan S., Yang Q., Liu J. An experimental investigation on heat transfer performance of pulsating heat pipe. *Journal of Mechanical Science and Technology*, 2020, vol. 34, pp. 425–433. DOI: 10.1007/s12206-019-1241-x.

5. Ganapathy V. *Steam generators and waste heat boilers: For process and plant engineers*. Boca Raton, CRC Press, 2014. 539 p. ISBN 9781138077683.

6. Zohuri B. *Application of compact heat exchangers for combined cycle driven efficiency in next generation nuclear power plants: A novel approach*. Cham, Springer Nature Link, 2015. 366 p. eISBN 978-3-319-23537-0. DOI: 10.1007/978-3-319-23537-0.

7. Bassols J., Kuckelkorn B., Langreck J., Schneider R., Veelken H. Trigeneration in the food industry. *Applied Thermal Engineering*, 2002, vol. 22 (6), pp. 595–602. DOI: 10.1016/S1359-4311(01)00111-9.

8. Šalić A., Tušek A., Zelić B. Application of microreactors in medicine and biomedicine. *Journal of Applied Biomedicine*, 2012, vol. 10 (3), pp. 137–153. DOI: 10.2478/v10136-012-0011-1.

9. Sharma A., Tyagi V.V., Chen C.R., Buddhi D. Review on thermal energy storage with phase change materials and applications. *Renewable and Sustainable Energy Reviews*, 2009, vol. 13 (2), pp. 318–345. DOI: 10.1016/j.rser.2007.10.005.

10. Ameen A. *Refrigeration and air conditioning*. PHI Learning Pvt. Ltd., 2006. 512 p. ISBN 8120326717. ISBN 978-8120326712.

11. Oliet C., Oliva A., Castro J., Pérez-Segarra C.D. Parametric studies on automotive radiators. *Applied Thermal Engineering*, 2007, vol. 27 (11), pp. 2033–2043. DOI: 10.1016/j.applthermaleng.2006.12.006.

12. Heldman D., Moraru C.E., eds. *Encyclopedia of agricultural, food, and biological engineering*. 2nd ed. Boca Raton, CRC Press, 2010. DOI: 10.1201/9780429257599.

13. Coker A.K. Introduction. Coker A.K. *Petroleum refining design and application handbook*. John Wiley & Sons, 2018, ch. 1, pp. 1–6. ISBN 978-1-119-25710-3. DOI: 10.1002/9781119257110.ch1.

14. Coker A.K. Thermodynamic properties of petroleum and petroleum fractions. Coker A.K. *Petroleum refining design and application handbook*. John Wiley & Sons, 2018, ch. 4, pp. 63–110. DOI: 10.1002/9781119257110.ch4.

15. Beddoes J., Bibby M. *Principles of metal manufacturing processes*. Butterworth-Heinemann, 1999. DOI: 10.1016/B978-0-340-73162-8.X5000-0.

16. Abu Rowin W., Xia Y., Wang S., Hutchins N. Accurately predicting turbulent heat transfer over rough walls: a review of measurement equipment and methods. *Experiments in Fluids*, 2024, vol. 65, p. 86. DOI: 10.1007/s00348-024-03812-1.

17. Qu W., Ma H.B. Theoretical analysis of startup of a pulsating heat pipe. *International Journal of Heat and Mass Transfer*, 2007, vol. 50 (11–12), pp. 2309–2316. DOI: 10.1016/j.ijheatmasstransfer.2006.10.043.

18. Chen X., Lin Y., Shao S., Wu W. Study on heat transfer characteristics of ethane pulsating heat pipe in middle-low temperature region. *Applied Thermal Engineering*, 2019, vol. 152, pp. 697–705. DOI: 10.1016/j.applthermaleng.2019.02.125.

19. Singh S., Singh S.K., Mali H.S., Dayal R. Numerical investigation of heat transfer in structured rough microchannels subjected to pulsed flow. *Applied Thermal Engineering*, 2021, vol. 197, p. 117361. DOI: 10.1016/j.applthermaleng.2021.117361.

20. Wu H.-W., Lay R.-F., Lau C.-T., Wu W.-J. Turbulent flow field and heat transfer in a heated circular channel under a reciprocating motion. *Heat and Mass Transfer*, 2004, vol. 40 (10), pp. 769–778. DOI: 10.1007/s00231-003-0464-6.

21. Lin T.-Y., Kandlikar S.G. An experimental investigation of structured roughness effect on heat transfer during single-phase liquid flow at microscale. *Journal of Heat Transfer*, 2012, vol. 134, p. 101701. DOI: 10.1115/1.4006844.

22. Lu H., Xu M., Gong L., Duan X., Chai J.C. Effects of surface roughness in microchannel with passive heat transfer enhancement structures. *International Journal of Heat and Mass Transfer*, 2020, vol. 148, p. 119070. DOI: 10.1016/j.ijheatmasstransfer.2019.119070.

23. Croce G., D'agaro P., Nonino C. Three-dimensional roughness effect on microchannel heat transfer and pressure drop. *International Journal of Heat and Mass Transfer*, 2007, vol. 50 (25), pp. 5249–5259. DOI: 10.1016/j.ijheatmasstransfer.2007.06.021.

24. Gerrard J.H. An experimental investigation of pulsating turbulent water flow in a tube. *Journal of Fluid Mechanics*, 1971, vol. 46 (1), pp. 43–64. DOI: 10.1017/S0022112071000399.

25. Clamen M., Minton P. An experimental investigation of flow in an oscillating pipe. *Journal of Fluid Mechanics*, 1977, vol. 81 (3), pp. 421–431. DOI: 10.1017/S0022112077002146.

26. Shemer L., Wygnanski I., Kit E. Pulsating flow in a pipe. *Journal of Fluid Mechanics*, 1985, vol. 153, pp. 313–337. DOI: 10.1017/S0022112085001276.

27. Eckmann D.M., Grotberg J.B. Experiments on transition to turbulence in oscillatory pipe flow. *Journal of Fluid Mechanics*, 1991, vol. 222, pp. 329–350. DOI: 10.1017/S002211209100112X.

28. Ohmi M., Usui T., Tanaka O., Toyoma M. Pressure and velocity distributions in pulsating turbulent pipe flow. Part 2. Experimental investigations. *Bulletin of JSME*, 1976, vol. 19 (134), pp. 951–957. DOI: 10.1299/jsme1958.19.951.

29. Iguchi M., Park G., Koh Y. The structure of turbulence in pulsatile pipe flows. *KSME Journal*, 1993, vol. 7, pp. 185–193. DOI: 10.1007/BF02970963.

30. Genin L.G., Koval A.P., Manchkha S.P., Sviridov V.G. Hydrodynamics and heat transfer with pulsating fluid flow in tubes. *Thermal Engineering*, 1992, vol. 39 (5), pp. 251–255.

31. Einav S., Sokolov M. An experimental study of pulsatile pipe flow in the transition range. *Journal of Biomechanical Engineering*, 1993, vol. 115 (4A), pp. 404–411. DOI: 10.1115/1.2895504.

32. Carvalho Jr J.A. Behavior of solid particles in pulsating flows. *Journal of Sound and Vibration*, 1995, vol. 185 (4), pp. 581–593. DOI: 10.1006/jsvi.1995.0402.

33. Lu P.-C. Discussion: "Heat Transfer for Pulsating Laminar Duct Flow" (Siegel, R., and Perlmutter, M., 1962, ASME J. Heat Transfer, 84, pp. 111–122). *Journal of Heat Transfer*, 1962, vol. 84, pp. 111–122. DOI: 10.1115/1.3684308.

34. Faghri M., Javdani K., Faghri A. Heat transfer with laminar pulsating flow in a pipe. *Letters in Heat and Mass Transfer*, 1979, vol. 6 (4), pp. 259–270. DOI: 10.1016/0094-4548(79)90013-4.

35. Krishnan K.N., Sastri V.M.K. Heat transfer in laminar pulsating flows of fluids with temperature dependent viscosities. *Wärme- und Stoffübertragung*, 1989, vol. 24 (1), pp. 27–42. DOI: 10.1007/BF01599503.

36. Cho H., Hyun J. Numerical solutions of pulsating flow and heat transfer characteristics in a pipe. *International Journal of Heat and Fluid Flow*, 1990, vol. 11 (4), pp. 321–330. DOI: 10.1016/0142-727X(90)90056-H.

37. Kim S.Y., Kang B.H., Hyun J.M. Heat transfer from pulsating flow in a channel filled with porous media. *International Journal of Heat and Mass Transfer*, 1994, vol. 37 (14), pp. 2025–2033. DOI: 10.1016/0017-9310(94)90304-2.

38. Gül H. Experimental investigation of heat transfer in oscillating circular pipes: High frequencies and amplitudes. *Scientific Research and Essays*, 2013, vol. 8 (13), pp. 524–531. DOI: 10.5897/SRE12.721.

39. Dittus F., Boelter L. Heat transfer in automobile radiators of the tubular type. *International Communications in Heat and Mass Transfer*, 1985, vol. 12 (1), pp. 3–22. DOI: 10.1016/0735-1933(85)90003-X.

40. Winterton R.H.S. Technical notes: Where did the dittus and boelter equation come from? *International Journal of Heat and Mass Transfer*, 1998, vol. 41 (4–5), pp. 809–810. DOI: 10.1016/S0017-9310(97)00177-4.

41. McAdams W.H. *Heat transmission*. 3rd ed. New York, McGraw-Hill, 1954. ISBN 0070447993. ISBN 9780070447998.

42. Bagade P.M., Bhumkar Y.G., Sengupta T.K. An improved orthogonal grid generation method for solving flows past highly cambered aerofoils with and without roughness elements. *Computers and Fluids*, 2014, vol. 103, pp. 275–289. DOI: 10.1016/j.compfluid.2014.07.031.

43. Elshafei E.A.M., Safwat Mohamed M., Mansour H., Sakr M. Experimental study of heat transfer in pulsating turbulent flow in a pipe. *International Journal of Heat and Fluid Flow*, 2008, vol. 29 (4), pp. 1029–1038. DOI: 10.1016/j.ijheatfluidflow.2008.03.018.

44. Cebeci T., Bradshaw P. *Physical and computational aspects of convective heat transfer*. New York, Springer, 2012. DOI: 10.1007/978-1-4612-3918-5.

45. Kays W., Crawford M., Weigand B. *Convective heat and mass transfer*. McGraw-Hill, 2005. ISBN 0072468769. ISBN 978-0072468762.

46. Chung D., Hutchins N., Schultz M.P., Flack K.A. Predicting the drag of rough surfaces. *Annual Review of Fluid Mechanics*, 2021, vol. 53, pp. 439–471. DOI: 10.1146/annurev-fluid-062520-115127.

47. Alfarawi S., Abdel-Moneim S.A., Bodalal A. Experimental investigations of heat transfer enhancement from rectangular duct roughened by hybrid ribs. *International Journal of Thermal Sciences*, 2017, vol. 118, pp. 123–138. DOI: 10.1016/j.ijthermalsci.2017.04.017.

48. MacDonald M., Chan L., Chung D., Hutchins N., Ooi A. Turbulent flow over transitionally rough surfaces with varying roughness densities. *Journal of Fluid Mechanics*, 2016, vol. 804, pp. 130–161. DOI: 10.1017/jfm.2016.459.

49. Everts M., Ayres S.R., Mulock Houwer F.A., Vanderwagen C.P., Kotze N.M., Meyer J.P. The influence of surface roughness on heat transfer in the transitional flow regime. *Proceedings of the 15th International Heat Transfer Conference*. Begellhouse, 2014. DOI: 10.1615/IHTC15.cnv.008338.

50. Meyer J., Olivier J. Transitional flow inside enhanced tubes for fully developed and developing flow with different types of inlet disturbances: Part I – Adiabatic pressure drops. *International Journal of Heat and Mass Transfer*, 2011, vol. 54 (7), pp. 1587–1597. DOI: 10.1016/j.ijheatmasstransfer.2010.11.027.

51. Meyer J., Olivier J. Transitional flow inside enhanced tubes for fully developed and developing flow with different types of inlet disturbances: Part II – Heat transfer. *International Journal of Heat and Mass Transfer*, 2011, vol. 54 (7), pp. 1598–1607. DOI: 10.1016/j.ijheatmasstransfer.2010.11.026.

52. García A., Solano J.P., Vicente P.G., Viedma A. The influence of artificial roughness shape on heat transfer enhancement: Corrugated tubes, dimpled tubes and wire coils. *Applied Thermal Engineering*, 2012, vol. 35, pp. 196–201. DOI: 10.1016/j.applthermaleng.2011.10.030.

53. Mousa M.H., Miljkovic N., Nawaz K. Review of heat transfer enhancement techniques for single phase flows. *Renewable and Sustainable Energy Reviews*, 2021, vol. 137, p. 110566. DOI: 10.1016/j.rser.2020.110566.

54. Everts M., Meyer J.P. Heat transfer of developing and fully developed flow in smooth horizontal tubes in the transitional flow regime. *International Journal of Heat and Mass Transfer*, 2018, vol. 117, pp. 1331–1351. DOI: 10.1016/j.ijheatmasstransfer.2017.10.071.

55. Kobayashi S., Inokuma K., Murata A., Iwamoto K. Effects of flow pulsation and surface geometry on heat transfer performance in a channel with teardrop-shaped dimples measured by transient technique. *ASME Journal of Heat and Mass Transfer*, 2024, vol. 146, p. 072001. DOI: 10.1115/1.4065117.

56. Abdelfattah M., Aziz M.A., Maghrabie H.M. Numerical analysis of heat transfer and fluid flow structures of jet impingement on a flat plate with different shapes of roughness elements. *Numerical Heat Transfer, Part A: Applications*, 2024, pp. 1–26. DOI: 10.1080/10407782.2024.2379032.

57. *Ansys Fluent Theory Guide*. ANSYS, Inc., 2021.

58. Nikuradse J. *Laws of flow in rough pipes*. *NACA Technical Memorandums*, NACA-TM-1292. NACA, 1950. 62 p.

59. Cebeci T., Bradshaw P. *Momentum transfer in boundary layers*. Washington, Hemisphere Pub. Corp., 1977. 407 p. ISBN 0070103003. ISBN 9780070103009.

60. Nishandar S.V., Pise A.T., Bagade P.M., Gaikwad M.U., Singh A. Computational modelling and analysis of heat transfer enhancement in straight circular pipe with pulsating flow. *International Journal on Interactive Design and Manufacturing (IJIDeM)*, 2024, vol. 19 (3), pp. 1951–1969. DOI: 10.1007/s12008-024-01907-x.

61. Dwivedi R., Somatkar A., Chinchanikar S. Modeling and optimization of roller burnishing of Al6061-T6 process for minimum surface roughness, better microhardness and roundness. *Obrabotka metallov (tekhnologiya, oborudovanie, instrumenty)* = *Metal Working and Material Science*, 2024, vol. 26, no. 3, pp. 52–65. DOI: 10.17212/1994-6309-2024-26.3-52-65.

Conflicts of Interest

The authors declare no conflict of interest.